
Peptide-Spectra Matching from Weak Supervision

Samuel S. Schoenholz
Google Brain
schsam@google.com

Sean Hackett
Calico Life Sciences LLC
sean@calicolabs.com

Laura Deming
Longevity Fund
ldeming.www@gmail.com

Eugene Melamud
Calico Life Sciences LLC
eugene@calicolabs.com

Navdeep Jaitly
Google Brain
ndjaitly@google.com

Fiona McAllister
Calico Life Sciences LLC
fiona@calicolabs.com

Jonathon O'Brien
Calico Life Sciences LLC
obrienj@calicolabs.com

George Dahl
Google Brain
gdahl@google.com

Bryson Bennett
Calico Life Sciences LLC
bryson@calicolabs.com

Andrew M. Dai
Google Brain
adai@google.com

Daphne Koller
Insitro*
daphne@insitro.com

Abstract

As in many other scientific domains, we face a fundamental problem when using machine learning to identify proteins from mass spectrometry data: large ground truth datasets mapping inputs to correct outputs are extremely difficult to obtain. Instead, we have access to imperfect hand-coded models crafted by domain experts. In this paper, we apply deep neural networks to an important step of the protein identification problem, the pairing of mass spectra with short sequences of amino acids called peptides. We train our model to differentiate between top scoring results from a state-of-the-art classical system and hard-negative second and third place results. Our resulting model is much better at identifying peptides with spectra than the model used to generate its training data. In particular, we achieve a 43% improvement over standard matching methods and a 10% improvement over a combination of the matching method and an industry standard cross-spectra reranking tool. Importantly, in a more difficult experimental regime that reflects current challenges facing biologists, our advantage over the previous state-of-the-art grows to 15% even after reranking. We believe this approach will generalize to other challenging scientific problems.

1 Introduction

Historically, analysis of complex scientific data has been made possible by domain experts using theory and expert knowledge to create simple causal models that can be used to make inferences from measurements. In these cases, there is often no ground truth associated with the data and a great deal of effort goes into quantifying the performance of these hand-made models. Examples of this situation are widespread but include: scattering data in high-energy physics experiments [1], measurements from gravitational wave observatories [2], and cryo-electron microscopy [12]. The difficulty of quantitative evaluation complicates the use of machine learning at the cutting-edge of science.

*Work done while at Calico Life Sciences LLC.

Simultaneously, machine learning models based on deep neural networks have achieved impressive performance across a variety of tasks in the natural sciences in cases where ground truth is available. Some examples of these recent successes include predicting the properties of small molecules [10], predicting the properties of drugs [26] and materials [28], and predicting the local structure of proteins [5]. Ideally we would be able to achieve similar success even when using weaker supervision. In this work, we tackle this more general problem of weak supervision in the context of a scientific problem of practical importance: identifying proteins in biological samples from mass spectrometry measurements. Our approach is to leverage noisy labels from classical database matching algorithms to train a machine learning algorithm whose performance is *significantly* better than the tool used to construct the labels.

Answering fundamental questions in biology such as how cellular processes are regulated or how these processes are altered in disease requires an accurate picture of an organism’s biochemical state. Since most cellular processes of interest are implemented by proteins, the state of proteins in a cell is extremely relevant information if we want to understand how cells operate. Cells, however, are complex environments that contain large numbers of proteins. The inverse problem of identifying which proteins are present in a given cell is complex and has received a significant amount of attention. A crucial step in modern workflows involves associating short sequences of amino acids, called peptides, with readings from a mass spectrometer (which essentially produces a histogram of the different ways that the peptide can fragment). If these peptides can successfully be identified, then other models can reconstruct the protein population. Unfortunately, ground truth pairings between peptides and spectra are not readily obtained. Therefore, if machine learning is to be successful in this domain we must be able to use existing noisy labels to make progress.

The primary contributions of this manuscript are as follows. We first introduce a method for training general machine learning models to identify peptides corresponding to a given mass spectrum based on noisy labels from classical algorithms. We include a detailed discussion of pitfalls that can occur when attempting to apply deep learning methods in this framework along with solutions to avoid various modes of failure. Next, we introduce a family of models that we believe have a strong inductive bias towards the problem of matching sequences with histogram readouts. Finally, we discuss the performance of our model, show that it significantly outperforms classical approaches, and demonstrate that this performance gap widens as the problem becomes harder.

2 Related Work

Our paper shows how unlabeled mass spectral data can be assigned peptide labels using prior models and how new models can be trained from the generated labels. Such *weak*, *pseudo* and *self* labeling strategies are not new to the area of machine learning [19, 21, 22]. For example, Liao et al. [21] applies an existing model to YouTube videos to generate possible transcripts and filters out matches that are presumed to be bad. Good matches are used to train a subsequent model, producing improvements over the previous model. Pseudo-labeling has been used previously in mass spectrometry for retention time prediction with a neural network, where a dataset of peptide sequence, retention time pairs was generated from large datasets using stringent rules applied to SEQUEST results [25]. Percolator, an algorithm for peptide identification from mass spectrometry, also used a *pseudo* labelling strategy to train their model [17]. However, Percolator uses a fixed set of fairly high level features of the matches in their support vector machine, while this work uses deep learning strategies to discover features and scoring functions directly from the data – the mass spectrum itself. Additionally, a similar labeling strategy to that proposed here has been used in physics to identify defects in glasses from noisy measurements of relaxation events [27].

The use of deep learning models for mapping sequences to structured outputs is also well studied [32, 34, 23, 5]. Typically, however, such models are applied in a blackbox manner; in contrast, in this paper, we introduce an architecture that is partially a black-box, and is partially manually designed to reflect the structure of the peptide fragment problem — namely that the fragmentation pattern of a peptide is a sum of the fragmentation pattern of the N- and C-terminus subsequences of the peptide. However, our model is modular, and can be easily extended to other input structures, such as graphs (or chemical structures) using graph embeddings [20] and as a result can be applied to other mass spectrometry modalities such as metabolomics and scanning electron microscopy.

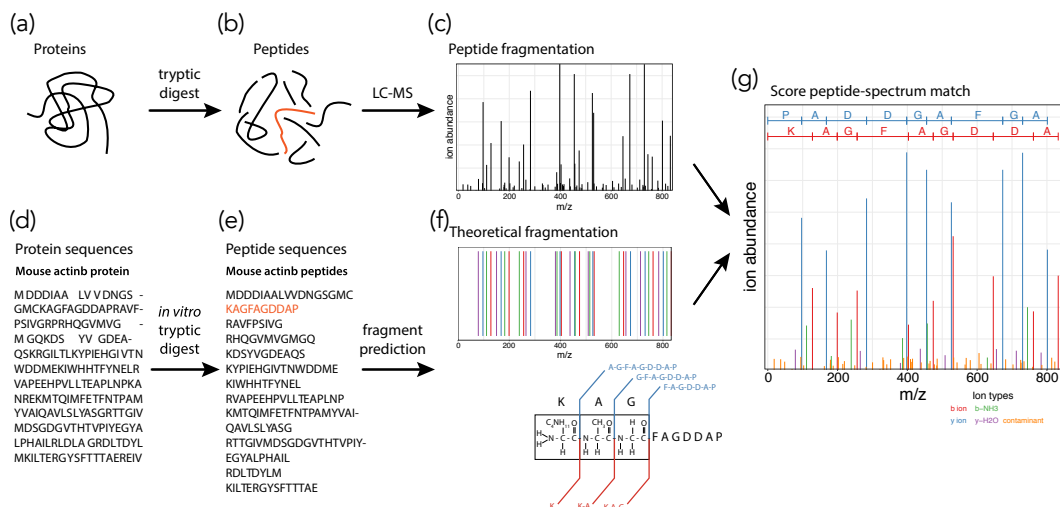


Figure 1: Overview of fragmentation matching in LC-MS proteomics. Experimental fragmentation spectra of unknown proteins (a) are generated by isolating individual peptides (b) and then fragmenting the peptide into pieces in a mass spectrometer (c). To narrow down the number of feasible candidates for a fragmentation event, the genome of the organism of interest (d) can be digested to yield a set of feasible peptides (e). Each peptide’s common fragments can be predicted based on its sequence, since peptides primarily fragment along the C-N bonds in the backbone and often lose either water or ammonia in the process (f). During the peptide-spectrum matching process an experimental fragmentation spectra is compared to the theoretical spectra of a candidate peptide to determine the most likely match (g).

Tran et al. [33] have previously applied deep learning to peptide-spectra matching. However, they focused on the *de novo* sequencing problem where the peptide search space is unconstrained and is consequently a substantially more difficult problem. While they demonstrated a substantial improvement over the state-of-the-art, results on the *de novo* sequencing remain too poor to be used in practice.

As an additional note, our method of comparing best match sequences to second and third-best sequence matches for a spectral output, might also be appropriate for hot-word matching models in speech recognition, where fixed length audio snippets are often compared to a set of candidate hot-words [4]. Another possible application of our model that identifies structured inputs with a distribution might be the association of crystal structures with data from scattering experiments [3].

2.1 Experimental Proteomics

In proteomics, the goal is to identify protein populations occurring in organisms. Here we give a brief summary of experimental proteomics. In the supplementary information we include a slightly more extensive description. Figure 1 shows a simplified schematic of a common pipeline for protein identification used in proteomics called liquid chromatography-mass spectrometry (LC-MS). Proteins from complex biological samples are isolated with biochemical techniques, and separated into less complex mixtures based on their properties (Figure 1a). These mixtures of proteins are digested into pieces called peptides (1b) and further separated by liquid chromatography based on their biochemical properties. The peptides are individually (hopefully) injected into a mass spectrometer and fragmented into smaller pieces. The mass to charge ratio of these fragments is then measured to produce a histogram of the relative intensities of the fragments (1c). The goal of a modern LC-MS pipeline is then to infer the original protein population from these histograms.

3 Methods

3.1 DeepMatch: A model for peptide-spectra matching

In this section, we will describe our model which we refer to as DeepMatch. Suppose we have scans from a mass spectrometer that we wish to associate with peptides. Generally a scan comes as a set of pairs (m_i, I_i) where m_i is the m/z (mass-to-charge ratio) of a peak in the spectrum and I_i is the measured intensity of the peak. We will discretize this measurement into M different m/z bins of width ΔM so that $M_i = M_{\min} + i\Delta M$ are the bin edges; thus the reading from the mass spectrometer will be represented by a vector $\hat{y} \in \mathbb{R}_{>0}^M$ such that \hat{y}_i is the summed intensity at each bin. In these experiments $M = 3800$, $M_{\min} = 100$ Daltons, and $\Delta M = 0.5$ Daltons. We think of the mass spectrometer as measuring the distribution over all the different ways in which the peptide can fragment and the different m/z ratios that the fragments can have (either due to variable charges, neutral losses, etc). To this end we turn the intensity measurements into a probability distribution by normalizing the reading to give $\hat{p}_i = \hat{y}_i / \|\hat{y}\|_1$.

Simultaneously we can represent the peptide as a sequence of L (possibly modified) amino acids, $x_1 \cdots x_L$. We will typically use a one-hot encoding of the amino acids that we will augment with additional side information such as the mass of the peptide, the precursor charge, the retention time, and the hydrophobicity. Thus, we embed each amino acid $x_a \in \mathbb{R}^A$.

To train our model, we will construct a dataset of sequence – distribution pairs. Some of these pairs will be real associations and have an assigned label $t = 1$. Other pairs will be fake and have a label $t = 0$. Our goal will be to train a model that can distinguish between the real and fake examples.

We propose a model family with four distinct pieces that we discuss schematically here. In the supplementary information we discuss several different components that we explored for each piece of the network. Note, that different components can be swapped out easily as long as their input / output dimensions agree.

Fragment Representation: A function $F : \mathbb{R}^{L \times A} \rightarrow \mathbb{R}^{(L+1) \times F}$, maps sequences of amino acids to a “fragment” representation, of dimension F , that we hope will contain information about the probabilities of different fragmentations as well as their m/z values. We will write $(f_1, \dots, f_{L+1}) = F(x_1, \dots, x_L)$. Typically we will take F to be a bidirectional-LSTM [13]. If we wished to try to apply these methods to molecules that could not naturally be expressed as a sequence we could also have F be an MPNN [20, 10].

Spectral Representation: The second piece of our model is a composition of a fully connected neural network, $Y : \mathbb{R}^{(L+1) \times F} \rightarrow \mathbb{R}^{M \times H}$, which maps the fragment representation to a “spectral” representation with embedding dimension H . This spectral representation associates the different fragments with m/z bins. Generally we will write $(y_1, \dots, y_M) = Y(f_1, \dots, f_{L+1})$. See the supplementary information for more details.

Readout: Next, our model will compare the fragment representation of the peptide, y_i , with the measured spectrum \hat{y}_i to arrive at a score, $s \in \mathbb{R}$ using a score function $S : \mathbb{R}^{M \times (H+1)} \rightarrow \mathbb{R}$. We will typically write $s = S(\hat{y}, y)$. We will typically use the normalized version of the spectrum, \hat{p}_i instead of the raw intensities. In practice we will let S be based on the VGG network architecture [29] similar to those found in image recognition systems.

Loss: Finally, we will compute a per-example loss that we hope to extremize using our score. We will take this to be a cross entropy loss. To define the cross entropy loss we construct a probability of a match being real using the score as a logit, $\hat{p} = \sigma(s)$. We can then define the cross-entropy, $L = -\sum_i [p_i \log \hat{p}_i + (1 - p_i) \log(1 - \hat{p}_i)]$ where p_i can be the label, t_i . However, we will often have information about how likely a given sequence-distribution pair is of being real. In that case p_i can be set to this likelihood to give a form of label smoothing that we have found to be helpful in practice.

We can see a diagram of this class of models in Figure 2. We will go into details on the specific choices of these components for the problem of peptide-spectrum identification in the supplementary information.

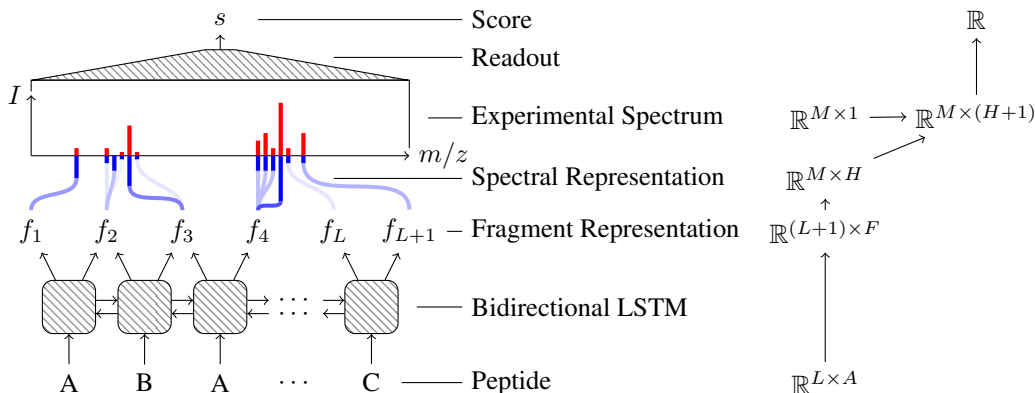


Figure 2: Components of DeepMatch along with shapes.

3.2 Weak Supervision

As discussed above, a fundamental issue in the application of deep learning to problems across a variety of domains is the lack of ground truth labels. Here, we offer a discussion of this problem that ought to be general enough to be applicable in a wide range of situations.

Suppose we have a generative process so that a distribution, $p(y|x)$, is generated by a latent variable x . In the current setting, x will be a sequence of amino acids and $p(y|x)$ will be the mass spectrum that results from fragmenting that sequence. Further, let us assume that we have access to a noisy labeling function f that assigns scores to sequence-distribution pairs. We take the noisy labeling function to be well behaved in the sense that if $f(x, q(y)) > f(x, q'(y))$ then x is more likely to have generated $q(y)$ than $q'(y)$.

For a given empirical distribution $q(y)$, we can therefore identify the most likely sequence to have produced $q(y)$ by extremizing, $\hat{x} = \operatorname{argmax}_x f(x, q(y))$. This, in turn gives an associated score for the pair, $\hat{s} = f(\hat{x}, q(y))$. Thus, for any dataset of unlabeled distributions we can construct a labeled dataset where we additionally pair each example with an associated score. To construct our training set, we then choose a threshold s^* and pick only those elements of the dataset whose score is greater than s^* . By increasing the threshold, this allows us to tune between dataset size and match confidence. In cases where the score can be explicitly associated with a probability of a correct match, we can use this probability to perform label-smoothing as discussed above.

4 Methods

4.1 Peptide Spectrum Matching

In order to make use of the quantitative information present in LC-MS proteomics data, we need to know which peptides, and by extension which proteins, were detected in a sample. This occurs by predicting which peptide generated each of the many fragmentation spectra produced in an experiment. Fragmentation spectra are informative of peptide sequence because peptides fragment in a probabilistic way, dependent on their sequence. For peptides that fragment cleanly, and produce a high-quality spectra, the masses of individual amino acids in the sequence can essentially be read-off from the spacing between prominent neighbouring peaks. However, most peptides do not fragment or ionize equally well at each bond; this can often be a function of their sequence (such as electron-affinity of subsequences). Thus some fragments will be missing in spectra. Further, contamination from other peptides of the same parent m/z can produce noisy peaks, making the matching of fragmentation spectra to peptide sequences an ongoing challenge. While knowledge of simple fragmentation patterns is well known, one of our primary goals from this paper is to learn discriminative models of fragmentation patterns that improve identification, using recurrent sequence models such as LSTMs. Here, we offer a brief account of current techniques for associating peptides with spectra with reference to Figure 1. However, see Steen and Mann [30] for a more detailed account.

To solve the matching problem, classical approaches first construct a list of possible proteins present in the sample (Figure 1d). They then use this list to simulate a tryptic digest and construct a superset of plausible peptide sequences (1e). For a given spectrum, a small set of plausible candidates are constructed based on knowledge of the parent protein’s mass and charge. Each of these plausible candidates are then scored against the mass spectrum (1g). After having scored all plausible candidates, the highest scoring peptide is referred to as the peptide-spectrum match (PSM).

One of the most popular algorithms for scoring the agreement of a fragmentation spectra and a candidate peptide is the SEQUEST/COMET algorithm [7, 8]. The algorithm explicitly enumerates the theoretically possible fragments for any given peptide and uses a modified cross-correlation to evaluate the extent of agreement between expected and observed mass-to-charge ratios of the fragments (1f). However, due to the complexity of the fragmentation process, these methods do not do a good job of taking into account the relative abundances of the different possible fragments. Based on a suite of factors known to affect ion formation, we expect that the structure of a peptide will greatly impact the relative abundances of different fragments [14, 11]. A motivation for our deep learning architecture is to allow the model to encode information which is underutilized by conventional algorithms.

The peptide which best matches a fragmentation spectra may nevertheless be incorrect, especially when the score of the match is poor. In practice it is often desirable to estimate the rate at which PSMs of a given score are false-positives. This is called the false discovery rate ($FDR = \mathbb{E}[\frac{FP}{FP+TP}]$) [31] and it can be estimated in the following way [6, 17]. First, a large set of “dummy” candidate peptides are scored against the spectra in the same process as outlined above. These dummy peptides are generated by reversing the genome and then simulating the same tryptic digest as is applied to the forward genome. These dummy peptides will be statistically similar to the original set, but we can say with high confidence that they will not be present in nature. Each fragmentation spectra is scored against all viable real and dummy peptides and the top-ranked PSM is saved.

At low scores where there is little overlap between the observed and theoretical spectrum, we expect the rate at which dummy peptides are identified as a PSM to approach their relative abundance in the set of candidates. Typically, researchers would like to identify a score cutoff such that scores higher than the cutoff have a FDR of less than 1%. This can be found by the ratio of dummy to all peptides in the right-tail of the score distribution. In practice, a second round of re-ranking algorithms such as Percolator [15] are used to aggregate results across across many PSMs by using a linear-classifier to distinguish real and dummy peptides based on COMET scores and additional features.

4.2 Weak Supervision For Peptide-Spectrum Matching

We now discuss weak supervision in the context of the peptide-spectrum matching problem. We will first introduce a proxy task that we use to train our model, then we will discuss how we evaluate our model’s performance. The strong ability of deep learning models to memorize data means that there are a number of potential pitfalls especially around traditional evaluation methods for these models.

4.2.1 The Proxy Task

We consider a proxy task that is intimately related to the problem of peptide-spectra matching. As discussed above, an existing search algorithm (in this case COMET) is applied to a dataset of spectra to attain, for each spectrum, a set of cross-correlation scores for each of the candidate peptides considered [8]. We use Percolator to rescore the data. As in the general case, this gives us a score for each peptide-spectrum match and the probability of a true match increases monotonically with the score. In this case, we may additionally explicitly estimate an error probability for each PSM [15, 16]. We then construct a training set from the top- X (in this case $X = 3$) scoring peptides for spectra with an error probability $q \leq q^*$ (in this case $q^* = 50\%$). For each spectrum we assign the top-1 peptide a label $t = 1$ and the rest of the peptides a label $t = 0$. The 2nd and 3rd top ranked matches are used as negative examples.

There is some subtlety when defining negative examples since it is easy to select negatives that are too easy for DeepMatch to distinguish. By selecting the candidates that caused as much confusion as possible for COMET, we know that the theoretical fragmentations for our positive and negative examples correlate with the measured spectrum. While ours is not a unique choice, it is one that we have found works well in practice.

4.2.2 Model Selection and Evaluation

To evaluate our model and perform hyperparameter selection we use the previously discussed competitive real-decoy peptide searches [6, 17]. Thus, unlike in the case of training, we evaluate our model by scoring all the fragmentation events in an entire dataset. For each spectrum, we consider an identical set of candidate peptides to that assembled by COMET. We use our model to compute a score for each candidate paired separately with the spectrum. We then report the PSMs for each fragmentation spectra. To summarize the error in our model, we compute the number of PSMs at 1% FDR as described in section 4.1.

While the decoy method is on solid footing when applied to classical peptide-spectrum matching algorithms, for many choices of hyperparameters deep learning models will strongly tend to memorize peptides that it has seen. When such models are applied to the decoy method they perform exceptionally well, since they will preferentially select peptides that they have seen during training (which are all, by construction, real peptides). To get around this, we split our training and testing sets into different folds such that each fold contains spectra that were matched with a different disjoint subset of the total set of peptides. We then train our model on a subset of the folds and compute the number of peptides at 1% FDR on the remaining folds. When we perform our evaluation, we use a culled set of candidates that excludes any peptides that may have been seen during training. In this case, models that memorize peptides cannot subvert the decoy method and so this is a well defined metric that can be used in hyperparameter tuning.

To ensure that our models are not overfitting, we compare the number of peptides identified at 1% FDR using the full set of candidates compared to the culled set of candidates. If these two quantities are similar then our model does not manipulate the metric significantly and we can proceed with confidence. Another test for overfitting is to check that at low scores the false-discovery rate approaches N_{real}/N . Since at low scores there is very little useful information from the spectra, DeepMatch should identify decoys at the rate given by their fraction of the overall candidates.

5 Experiments

We take the best models after hyperparameter tuning and train them on data collected from several different species². For each species we assemble a list of candidate peptides by direct enumeration. The size of this candidate list depends on the species in question but generally varies between 10^9 and 10^{10} distinct peptide sequences whose length is between 5 and 40. We use 3800 bins to represent the mass spectrum. We then evaluate the model’s performance on unseen datasets and compare the results to COMET. For a brief description of the datasets used see the supplementary information. Our hyperparameter search identified the best DeepMatch model to have a single layer bidirectional LSTM with hidden dimension 600 and a spectral embedding of dimension 60.

We compare the distribution of scores found by our network to the distribution identified by COMET. These distributions are shown in Figure 3. We notice that by eye the distribution of scores identified

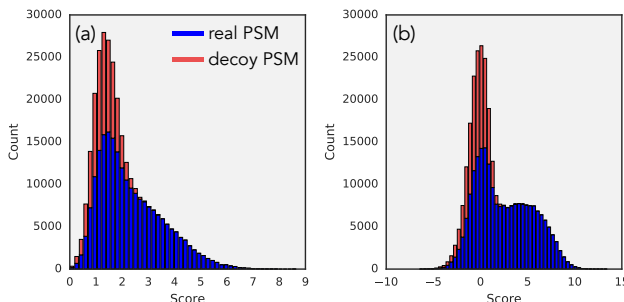


Figure 3: **The distribution of scores for peptide-spectra matches.** These scores are colored by whether or not they were real peptide-spectra matches or decoys for (a) COMET (b) DeepMatch.

²We intend to open-source the model and hyperparameters. More details are in the supplementary information.

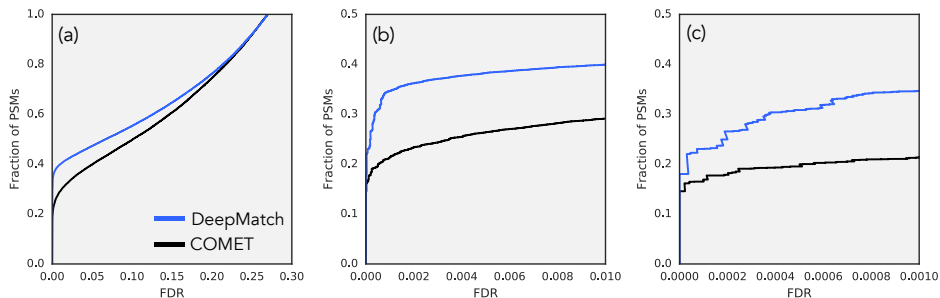


Figure 4: **A comparison between DeepMatch and COMET using the FDR metric.** The different figures show the same plot (a) for the full range of FDRs, (b) for FDRs up to 1%, and (c) for FDRs up to 0.1%.

by DeepMatch appears significantly more bimodal than the scores identified by COMET. We offer some analysis showing that our network’s scores are well behaved in the supplementary information.

DeepMatch is significantly more successful at correctly identifying peptide-spectrum matches. We observe in Figure 4 the number of peptide-spectrum matches at different FDRs. We observe that DeepMatch’s performance dominates COMET across FDRs. Moreover, zooming in to very low false-discovery rates we see that DeepMatch monotonically outperforms COMET which implies that DeepMatch is well behaved at high scores. At 1% FDR, we observe a 42% improvement in the number of spectra matched to peptides.

Search Algorithm	Fraction Matched At 1% FDR	
	Mouse	Yeast
COMET	29%	36%
DeepMatch	40%	47%
DeepMatch (No LSTM)	39%	45%
DeepMatch (Shallow Readout)	34%	43%

Table 1: A summary of our model’s performance as well as some baselines.

The results above show that DeepMatch significantly outperforms COMET as measured by the number of PSMs at 1% FDR as measured by the decoy search method. However, as we discussed above, the decoy search method gives an estimate of the FDR that can easily be manipulated if care is not taken. To confirm these results, we used DeepMatch to find PSMs on the ProteomeTools dataset [36]. ProteomeTools is a large synthetic dataset where ground truth labels are known and so the FDR may be computed directly.

Search Algorithm	Estimated FDR	Correct	Incorrect	True FDR
DeepMatch	1%	481638	5449	1.1%
COMET	1%	374371	4633	1.5%

Table 2: A comparison of the FDR as measured using the decoy search method and measured against ground truth labels.

Table 2 shows the results of this comparison. To do this, we score a number of 50 different samples from ProteomeTools using DeepMatch and COMET and we enumerate the PSMs identified at 1% FDR as measured by the decoy search method. Among this subset of peptides, we then compute the FDR using the ground truth labels. We observe strong agreement between the estimated FDR using the decoy search method and the true FDR.

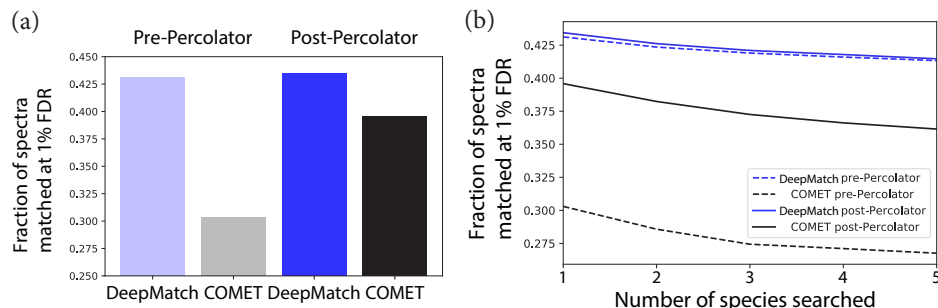


Figure 5: **Performance of DeepMatch and COMET pre- and post-Percolator.** (a) Fraction of spectra that are matched to a peptide at a 1% FDR when using COMET or DeepMatch for peptide-spectrum matching and optional recalibration using Percolator. (b) When searching spectra against an inflated list of target peptides (derived from additional species) the performance of DeepMatch models decay slower than COMET with or without Percolator.

Percolator greatly improves the performance of COMET and barely influences the performance of DeepMatch. Nevertheless the performance of DeepMatch over COMET with Percolator applied is still substantial. The number of spectra that can be identified at a 1% FDR is increased by 10% when using DeepMatch over a combination of COMET and Percolator (Figure 5a). In many biological applications, the set of candidate peptides is significantly larger than the setting considered here. To test our model’s performance in this regime we combined the candidate peptides from a number of species together. Since these additional candidate peptides will rarely be found in samples from mice, searching additional peptides should hurt our ability to detect true PSMs. However, we see little decay in the ability to recover matching with DeepMatch but a larger drop in performance when using COMET with or without Percolator. When searching five species simultaneously the pre-Percolator improvement of DeepMatch over COMET jumps to 54% and the improvement of our network over COMET and Percolator rises to 15%.

6 Conclusion

In this work we have introduced a method for training general machine learning models to identify peptides corresponding to a given mass spectrum based on noisy labels from classical algorithms. This can be used to study a class of inference problems in which an unknown sequence generates a distribution. We have additionally included a general discussion of a technique that can be used to leverage noisy labels to train our models to higher accuracy than the labels they were trained on. We observe strong performance on the important scientific problem of peptide-spectra matching and we believe that these techniques will be of broad use across a range of applications in the natural sciences.

Supplementary Material

6.1 Experimental Proteomics

Biological studies often require analyses of samples containing over 10,000 proteins. The prevailing technology for summarizing the broad-scale biological state – what proteins are present, if and how they are modified with post-translational modifications (PTMs), and how they vary across conditions – is Liquid chromatography-mass spectrometry (LC-MS) based proteomics. To understand how this feat is achieved, we will briefly describe the experimental generative process of an LC-MS proteomics experiment before tying this to the inverse problem that mass spectrometry search engines solve.

Proteins are linear chains of 100-1000s amino acids. There are 20 of these amino acids which are shared by nearly all organisms. Each gene forms one-or-more proteins and the sequence of nucleotides in a gene determines the sequence of amino acids in its protein(s). Some amino acids in an intact protein may be further processed (e.g., through the addition of a phosphate or methyl group) altering both the size and function of the modified amino acid.

Intact proteins are too large and complex to be analyzed by mass spectrometry, so most LC-MS proteomics experiments first digest intact proteins into 10-100s of short chemically-similar peptides composed of typically between 8 and 30 amino acids. This digestion utilizes an enzyme, such as Trypsin, which cuts proteins at specific positions, in order to break the protein into a small number of predictable fragments. Having digested 10,000+ proteins into ~ 100 peptides, there will now be $\sim 1,000,000$ distinct peptides present in a sample, which researchers want to separately detect and quantify.

The goal of an LC-MS proteomics experiment is to first chemically separate distinct peptides and then to physically separate, isolate and fragment each peptide for the purpose of identification and quantification. Distinct peptides are first separated based on their chemical properties primarily through liquid chromatography. In liquid chromatography, peptides are passed through a chromatography column and the time that it takes the peptide to reach the end of the column will be determined by specific chemical properties of the peptide. Thus, at each point in time, a subset of the entire peptide pool will elute from the column and this subset of peptides will be further separated using mass spectrometry. In the mass spectrometer, peptides will be ionized and then precisely distinguished based on their mass-to-charge (m/z) ratio. This generates a spectra which pairs a set of m/z ions with their associated ion current (abundance). These resolved peptides are finally isolated and then fragmented to generate a fragmentation spectra. A LC-MS proteomics experiments will generate $>10,000$ of such fragmentation spectra, and one of the chief challenges in computationally processing the resulting data is the "peptide-spectrum matching problem": attributing a peptide identity to each fragmentation spectra.

The traditional method for inferring what proteins were present in a sample, from the collection of mass spectra is to use a search engine such as SEQUEST[7], X!Tandem[9] or Mascot[24]. These search engines translate a database of genomic sequences from organisms being studied into protein sequences and digest them *in-silico* using known digestion rules, to create an index of peptides. A short set of candidate peptide matches is generated for each mass spectrum from the peptide index using the m/z values of the parent ions that were chosen for fragmentation and the mass of the peptides (using different possible integer charge values – usually 1-4, or determined by interpreting the charge of the parent ion, through the mass spectrum itself). Each candidate match is scored by generating a theoretical fragmentation spectrum and matching it to the observed one. Different search engines differ in how the theoretical fragmentation pattern is generated, and how the scoring functions are computed. However, for the most part, these fragmentation patterns used have been relatively simplistic – assuming all theoretical peaks are observed, and with equal intensity – when, in fact, peptide fragmentation is quite probabilistic, and depends on a variety of factors, such as the sequence of the peptide. This is the main limitation we tackle in this paper using the available datasets to learn a good scoring function and a predictive model for the fragmentation patterns.

Once candidate peptides matches are generated, they can be further filtered out by using manual or automated rules. Manual rules often use criterion based on numbers of peptides per proteins, while automated rules can use algorithms such as Protein Prophet [18] or Percolator[15] to further filter results from the first pass search. Percolator uses a support vector machine (SVM) to automatically train a second model on search results from the first pass search on a database with real peptides and decoy peptides (generated from a fake database – usually, a reversed protein dataset). The SVM is trained to separate high scoring matches from the forward direction sequence (label = 1) from the high scoring matches from the reverse direction (label = 0). The features used by Percolator as generally high level features of the matches, such as m/z difference between parent ion and theoretical m/z . The trained SVM is then used to clean up results from the first pass. Such a strategy can of course be used to clean up results from our methods as a second pass.

6.2 Model Components

We will now discuss a number of different components that we considered within our overall model family. Note that each of the four pieces above can be changed separately while adhering to the same overall structure as long as the dimension of the input and output are compatible.

6.2.1 The Fragment Representation

We propose two different methods of converting the amino acid representation into a fragment representation.

1. Trivial Representation:

As a baseline, we propose a trivial embedding where the amino acid representation is converted into a fragment representation via a projection. To do this we take $F : \mathbb{R}^{L \times A} \rightarrow \mathbb{R}^{(L+1) \times 2A}$ defined by,

$$F(x_1, \dots, x_L) = \begin{pmatrix} x_1 & \dots & x_L & 0 \\ 0 & x_1 & \dots & x_L \end{pmatrix} \quad (1)$$

Thus, the fragment f_i corresponding to a breakage between amino acid $i - 1$ and i is given by the concatenation of the amino acid representation before and after the breakage.

2. LSTM Representation:

In principle, we would like the fragment representation to be able to model the fragmentation probabilities between different amino acids. However, these probabilities depend not only on the pair of amino acids on either side of the breakage point, but on the structure of the entire peptide. To this end, we propose using a deep bidirectional LSTM with K layers and hidden dimension $F/2$ to construct the fragment representation that can take into account this nonlocal information. In this case the fragment representation is defined by,

$$(z_1, \dots, z_L) = \text{Bi-LSTM}(x_1, \dots, x_L) \quad (2)$$

$$F(x_1, \dots, x_L) = \begin{pmatrix} z_1 & \dots & z_L & 0 \\ 0 & z_1 & \dots & z_L \end{pmatrix}. \quad (3)$$

6.2.2 The Spectral Representation

We propose two different methods of converting from the fragment representation to the spectral representation. In one case, we use theoretical knowledge about the possible ways that the peptide can fragment. The other approach is agnostic to the underlying physical process. While we see significantly stronger performance when we use theory to constrain the form of our model, the agnostic approach may be more suitable when an explicit fragmentation cannot be enumerated. We also note that there is some overhead computational cost in precomputing the possible fragments.

1. Agnostic Representation:

Here we use a fully-connected network $g : \mathbb{R}^F \rightarrow \mathbb{R}^M$ to map each of the fragment representation into a corresponding contribution to the spectral representation. Thus, we write

$$Y(f_1, \dots, f_{L+1}) = \sum_{\ell} g(f_{\ell}). \quad (4)$$

This representation has $H = 1$ and potentially offers more interpretability since it can be normalized and interpreted as a probability distribution. Unfortunately, we were unable to get good performance using an agnostic representation that did not take explicit fragmentation patterns into account at the time of writing.

2. Ion Representation:

In this case we wish to take into account the fact that physically there are a finite number of ways in which a peptide may fragment. For each peptide we therefore enumerate all possible ways that the fragmentation can occur along with the theoretical mass-to-charge ratio that the resulting fragment will have.

To construct this enumeration, we first note that fragmentation occurs via the breaking of a bond between two amino acids. Moreover, between each pair of amino acids there are a number of different ways in which the fragmentation can occur (with different associated theoretical masses). In our experiments we use the three most likely breakages yielding so-called “b”, “y”, and “a” ions. Additionally fragments can have different charges associated with them. In our case we consider charges $Z = 1, 2$. Finally, can also have different neutral losses associated with them (where a molecule dissociates from the peptide during fragmentation). In our case we consider fragments that have lost an NH_3 molecule or an H_2O molecule.

Together this gives a combinatorial number of different ways that each breakage may occur. We enumerate these different possibilities with integers $0 \leq c \leq C \equiv 18$. For each possible breakage we construct a fully connected neural network $g_c : \mathbb{R}^F \rightarrow \mathbb{R}^H$ for some hidden

dimension H . Note that since fragmentation may occur between any pair of amino acids, there are a total of $C(L - 1)$ ways that the peptide can be fragmented overall. We let m_{ic} be the mass/charge ratio of the fragment of type c that occurs between amino acid i and $i + 1$. We then define the ion representation by $G \in \mathbb{R}^{M \times H}$, where,

$$G_k = \sum_{\substack{(i,c) \\ \text{s.t.} \\ m_{ic} \in [M_k, M_{k+1}]}} g_c(f_i). \quad (5)$$

Note that since the total number of possible fragments is small compared to the number of m/z bins, G will typically be very sparse.

6.2.3 Readout

We consider two different readout networks.

1. Trivial Readout:

As a baseline, we consider a trivial readout where a fully-connected network is applied directly to the concatenated spectral representation. In this case the score is given by, $s = w(G)$ for some fully connected $w : \mathbb{R}^{M \times H} \rightarrow \mathbb{R}$.

2. VGG Readout:

In general, we would like our network to learn complex correlations between the empirical spectrum and the spectral representation. To that end we use a copy of the VGG network [29] that has been successful in computer vision models. Thus, we take $s = \text{VGG}(G)$.

6.3 Dataset Description

We consider data from a number of species taken from the ProteomeXchange database [35] containing raw spectra. In particular we considered the datasets PXD005953 (Mouse), PXD002801 (Mouse), PXD001334 (Yeast), PXD002875 (Yeast), PXD003033 (Yeast), PXD005253 (Human), and PXD003389 (Human). These datasets varied significantly in size with the smallest having around 30K scans and the largest having $\sim 10\text{M}$ scans. For each species we assemble a list of candidate peptides by direct enumeration. The size of this candidate list depends on the species in question but generally varies between 10^9 and 10^{10} distinct peptide sequences whose length is between 5 and 40. We discretize the mass spectra using bins between 100 Daltons and 2000 Daltons of width 0.5 Daltons. This gives us 3800 bins in our discretized mass spectrum.

6.4 Network Diagnostics

We show that both the network scores and the COMET scores display similar characteristics. To

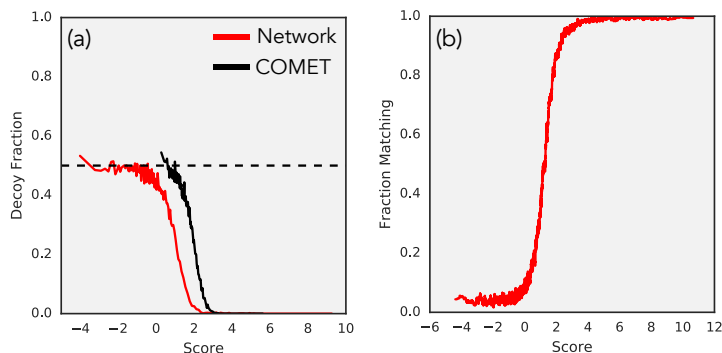


Figure 6: **Characteristics of the network scores.** (a) The fraction of decoys identified as top-1 peptide-spectra matches by the network and COMET. We see that at low scores both approach $\frac{1}{2}$ which is shown by a dashed line. (b) The fraction of peptide-spectrum matches that have agreement between the network at COMET. We see that at high scores the two methods almost always agree.

this end we show, in fig. 6 (a), the decoy fraction of top-1 peptide-spectrum matches as a function of the score assigned to the match. We see that we have successfully avoided selecting networks that memorize peptide data since our network and COMET both approach a decoy fraction of $\frac{1}{2}$ at low scores. Next, we calculate, as a function of the score, the fraction of peptide-spectrum matches where the network gave the same prediction as COMET. This is shown in fig. 6 (b). We see that at high scores the two assignments almost always agree. At low scores, the rate at which the two agree approaches the random value.

References

- [1] Georges Aad, B Abbott, J Abdallah, O Abidinov, R Aben, M Abolins, OS AbouZeid, H Abramowicz, H Abreu, R Abreu, et al. Combined measurement of the higgs boson mass in p p collisions at $\sqrt{s} = 7$ and 8 tev with the atlas and cms experiments. *Physical review letters*, 114(19):191803, 2015.
- [2] Benjamin P Abbott, Richard Abbott, TD Abbott, MR Abernathy, Fausto Acernese, Kendall Ackley, Carl Adams, Thomas Adams, Paolo Addesso, RX Adhikari, et al. Observation of gravitational waves from a binary black hole merger. *Physical review letters*, 116(6):061102, 2016.
- [3] Neil W Ashcroft, N David Mermin, and Sergio Rodriguez. Solid state physics, 1978.
- [4] Samy Bengio and Georg Heigold. Word embeddings for speech recognition. In *Fifteenth Annual Conference of the International Speech Communication Association*, 2014.
- [5] Akosua Busia and Navdeep Jaitly. Next-step conditioned deep convolutional neural networks improve protein secondary structure prediction. *CoRR*, abs/1702.03865, 2017. URL <http://arxiv.org/abs/1702.03865>.
- [6] Joshua E Elias and Steven P Gygi. Target-decoy search strategy for increased confidence in large-scale protein identifications by mass spectrometry. *Nature methods*, 4(3):207–214, March 2007.
- [7] Jimmy K Eng, Ashley L McCormack, and John R Yates. An approach to correlate tandem mass spectral data of peptides with amino acid sequences in a protein database. *Journal of The American Society for Mass Spectrometry*, 5(11):976–989, 1994.
- [8] Jimmy K Eng, Tahmina A Jahan, and Michael R Hoopmann. Comet: An open-source MS/MS sequence database search tool. *Proteomics*, 13(1):22–24, January 2013.
- [9] David Fenyő and Ronald C Beavis. A method for assessing the statistical significance of mass spectrometry-based protein identifications using general scoring schemes. *Analytical chemistry*, 75(4):768–774, 2003.
- [10] Justin Gilmer, Samuel S Schoenholz, Patrick F Riley, Oriol Vinyals, and George E Dahl. Neural message passing for quantum chemistry. *arXiv preprint arXiv:1704.01212*, 2017.
- [11] Ashley C Gucinski, Eric D Dodds, Wenzhou Li, and Vicki H Wysocki. Understanding and Exploiting Peptide Fragment Ion Intensities Using Experimental and Informatic Approaches. In *Proteome Bioinformatics*, pages 73–94. Humana Press, Totowa, NJ, 2010.
- [12] Richard Henderson and P Nigel T Unwin. Three-dimensional model of purple membrane obtained by electron microscopy. *Nature*, 257(5521):28, 1975.
- [13] Sepp Hochreiter and Jürgen Schmidhuber. Long short-term memory. *Neural Comput.*, 9(8):1735–1780, November 1997. ISSN 0899-7667. doi: 10.1162/neco.1997.9.8.1735. URL <http://dx.doi.org/10.1162/neco.1997.9.8.1735>.
- [14] Yingying Huang, Joseph M Triscari, Ljiljana Pasa-Tolic, Gordon A Anderson, Mary S Lipton, Richard D Smith, and Vicki H Wysocki. Dissociation behavior of doubly-charged tryptic peptides: correlation of gas-phase cleavage abundance with ramachandran plots. *Journal of the American Chemical Society*, 126(10):3034–3035, March 2004.
- [15] Lukas Käll, Jesse D Canterbury, Jason Weston, William Stafford Noble, and Michael J MacCoss. Semi-supervised learning for peptide identification from shotgun proteomics datasets. *Nature methods*, 4(11):923–925, November 2007.
- [16] Lukas Käll, John D Storey, Michael J MacCoss, and William Stafford Noble. Posterior Error Probabilities and False Discovery Rates: Two Sides of the Same Coin. *Journal of proteome research*, 7(1):40–44, December 2007.

- [17] Lukas Käll, John D Storey, Michael J MacCoss, and William Stafford Noble. Assigning significance to peptides identified by tandem mass spectrometry using decoy databases. *Journal of proteome research*, 7(1):29–34, January 2008.
- [18] Andrew Keller, Alexey I Nesvizhskii, Eugene Kolker, and Ruedi Aebersold. Empirical statistical model to estimate the accuracy of peptide identifications made by ms/ms and database search. *Analytical chemistry*, 74(20):5383–5392, 2002.
- [19] Dong-Hyun Lee. The simple and efficient semi-supervised learning method for deep neural networks. In *Workshop on Challenges in Representation Learning, ICML 2013*, 2013.
- [20] Yujia Li, Daniel Tarlow, Marc Brockschmidt, and Richard S. Zemel. Gated graph sequence neural networks. *CoRR*, abs/1511.05493, 2015. URL <http://arxiv.org/abs/1511.05493>.
- [21] Hank Liao, Erik McDermott, and Andrew Senior. Large scale deep neural network acoustic modeling with semi-supervised training data for youtube video transcription. In *Automatic Speech Recognition and Understanding (ASRU), 2013 IEEE Workshop on*, pages 368–373. IEEE, 2013.
- [22] David McClosky, Eugene Charniak, and Mark Johnson. Effective self-training for parsing. In *Proceedings of the main conference on human language technology conference of the North American Chapter of the Association of Computational Linguistics*, pages 152–159. Association for Computational Linguistics, 2006.
- [23] Aaron van den Oord, Sander Dieleman, Heiga Zen, Karen Simonyan, Oriol Vinyals, Alex Graves, Nal Kalchbrenner, Andrew Senior, and Koray Kavukcuoglu. Wavenet: A generative model for raw audio. *arXiv preprint arXiv:1609.03499*, 2016.
- [24] David N Perkins, Darryl JC Pappin, David M Creasy, and John S Cottrell. Probability-based protein identification by searching sequence databases using mass spectrometry data. *ELECTROPHORESIS: An International Journal*, 20(18):3551–3567, 1999.
- [25] Konstantinos Petritis, Lars J Kangas, Bo Yan, Matthew E Monroe, Eric F Strittmatter, Wei-Jun Qian, Joshua N Adkins, Ronald J Moore, Ying Xu, Mary S Lipton, et al. Improved peptide elution time prediction for reversed-phase liquid chromatography-ms by incorporating peptide sequence information. *Analytical chemistry*, 78(14):5026–5039, 2006.
- [26] Gisbert Schneider. Automating drug discovery. *Nature Reviews Drug Discovery*, 17:97 EP –, 12 2017. URL <http://dx.doi.org/10.1038/nrd.2017.232>.
- [27] Samuel S Schoenholz, Ekin D Cubuk, Daniel M Sussman, Efthimios Kaxiras, and Andrea J Liu. A structural approach to relaxation in glassy liquids. *Nature Physics*, 12(5):469, 2016.
- [28] Austin D Sendek, Qian Yang, Ekin D Cubuk, Karel-Alexander N Duerloo, Yi Cui, and Evan J Reed. Holistic computational structure screening of more than 12000 candidates for solid lithium-ion conductor materials. *Energy & Environmental Science*, 10(1):306–320, 2017.
- [29] Karen Simonyan and Andrew Zisserman. Very deep convolutional networks for large-scale image recognition. *arXiv preprint arXiv:1409.1556*, 2014.
- [30] Hanno Steen and Matthias Mann. The abc’s (and xyz’s) of peptide sequencing. *Nature reviews. Molecular cell biology*, 5(9):699–711, September 2004.
- [31] John D Storey and Robert Tibshirani. Statistical significance for genomewide studies. *Proceedings of the National Academy of Sciences of the United States of America*, 100(16):9440–9445, August 2003.
- [32] Ilya Sutskever, Oriol Vinyals, and Quoc V Le. Sequence to sequence learning with neural networks. In *Advances in neural information processing systems*, pages 3104–3112, 2014.
- [33] Ngoc Hieu Tran, Xianglilan Zhang, Lei Xin, Baozhen Shan, and Ming Li. De novo peptide sequencing by deep learning. *Proceedings of the National Academy of Sciences of the United States of America*, page 201705691, July 2017.
- [34] Oriol Vinyals, Łukasz Kaiser, Terry Koo, Slav Petrov, Ilya Sutskever, and Geoffrey Hinton. Grammar as a foreign language. In *Advances in Neural Information Processing Systems*, pages 2773–2781, 2015.
- [35] Juan A Vizcaíno, Eric W Deutsch, Rui Wang, Attila Csordas, Florian Reisinger, Daniel Rios, Jose A Dianes, Zhi Sun, Terry Farrah, Nuno Bandeira, et al. Proteomexchange provides globally coordinated proteomics data submission and dissemination. *Nature biotechnology*, 32(3):223, 2014.

- [36] Daniel P Zolg, Mathias Wilhelm, Karsten Schnatbaum, Johannes Zerweck, Tobias Knaute, Bernard Delanghe, Derek J Bailey, Siegfried Gessulat, Hans-Christian Ehrlich, Maximilian Weininger, Peng Yu, Judith Schlegl, Karl Kramer, Tobias Schmidt, Ulrike Kusebauch, Eric W Deutsch, Ruedi Aebersold, Robert L Moritz, Holger Wenschuh, Thomas Moehring, Stephan Aiche, Andreas Huhmer, Ulf Reimer, and Bernhard Kuster. Building ProteomeTools based on a complete synthetic human proteome. *Nature methods*, 14(3):259–262, March 2017.

Peptide-Spectra Matching from Weak Supervision

Supplementary Information

Anonymous Author(s)

Affiliation

Address

email

1 Experimental Proteomics

2 Biological studies often require analyses of samples containing over 10,000 proteins. The prevailing
3 technology for summarizing the broad-scale biological state – what proteins are present, if and how
4 they are modified with post-translational modifications (PTMs), and how they vary across conditions
5 – is Liquid-Chromatography Mass Spectrometry (LC-MS) based proteomics. To understand how this
6 feat is achieved, we will briefly describe the experimental generative process of an LC-MS proteomics
7 experiment before tying this to the inverse problem that mass spectrometry search engines solve.

8 Proteins are linear chains of 100-1000s amino acids. There are 20 of these amino acids which
9 are shared by nearly all organisms. Each gene forms one-or-more proteins and the sequence of
10 nucleotides in a gene determines the sequence of amino acids in its protein(s). Some amino acids in
11 an intact protein may be further processed (e.g., through the addition of a phosphate or methyl group)
12 altering both the size and function of the modified amino acid.

13 Intact proteins are too large and complex to be analyzed by mass spectrometry, so most LC-MS
14 proteomics experiments first digest intact proteins into 10-100s of short chemically-similar peptides
15 composed of typically between 8 and 30 amino acids. This digestion utilizes an enzyme, such as
16 Trypsin, which cuts proteins at specific positions, in order to break the protein into a small number
17 of predictable fragments. Having digested 10,000+ proteins into ~100 peptides, there will now be
18 ~1,000,000 distinct peptides present in a sample, which researchers want to separately detect and
19 quantify.

20 The goal of an LC-MS proteomics experiment is to first chemically separate distinct peptides and then
21 to physically separate, isolate and fragment each peptide for the purpose of identification and quan-
22 tification. Distinct peptides are first separated based on their chemical properties primarily through
23 liquid chromatography. In liquid chromatography, peptides are passed through a chromatography
24 column and the time that it takes the peptide to reach the end of the column will be determined by
25 specific chemical properties of the peptide. Thus, at each point in time, a subset of the entire peptide
26 pool will elute from the column and this subset of peptides will be further separated using mass
27 spectrometry. In the mass spectrometer, peptides will be ionized and then precisely distinguished
28 based on their mass-to-charge (m/z) ratio. This generates a spectra which pairs a set of m/z ions
29 with their associated ion current (abundance). These resolved peptides are finally isolated and then
30 fragmented to generate a fragmentation spectra. A LC-MS proteomics experiments will generate
31 >10,000 of such fragmentation spectra, and one of the chief challenges in computationally processing
32 the resulting data is the "peptide-spectrum matching problem": attributing a peptide identity to each
33 fragmentation spectra.

34 The traditional method for inferring what proteins were present in a sample, from the collection of
35 mass spectra is to use a search engine such as SEQUEST[?], X!Tandem[?] or Mascot[?]. These
36 search engines translate a database of genomic sequences from organisms being studied into protein
37 sequences and digest them *in-silico* using known digestion rules, to create an index of peptides. A
38 short set of candidate peptide matches is generated for each mass spectrum from the peptide index

39 using the m/z values of the parent ions that were chosen for fragmentation and the mass of the
 40 peptides (using different possible integer charge values - usually 1-4, or determined by interpreting
 41 the charge of the parent ion, through the mass spectrum itself). Each candidate match is scored by
 42 generating a theoretical fragmentation spectrum and matching it to the observed one. Different search
 43 engines differ in how the theoretical fragmentation pattern is generated, and how the scoring functions
 44 are computed. However, for the most part, these fragmentation patterns used have been relatively
 45 simplistic – assuming all theoretical peaks are observed, and with equal intensity – when, in fact,
 46 peptide fragmentation is quite probabilistic, and depends on a variety of factors, such as the sequence
 47 of the peptide. This is the main limitation we tackle in this paper using the available datasets to learn
 48 a good scoring function and a predictive model for the fragmentation patterns.

49 Once candidate peptides matches are generated, they can be further filtered out by using manual or
 50 automated rules. Manual rules often use criterion based on numbers of peptides per proteins, while
 51 automated rules can use algorithms such as Protein Prophet [?] or Percolator[?] to further filter
 52 results from the first pass search. Percolator uses a Support Vector Machine (SVM) to automatically
 53 train a second model on search results from the first pass search on a database with real peptides
 54 and decoy peptides (generated from a fake databaset –usually, a reversed protein dataset). The SVM
 55 is trained to separate high scoring matches from the forward direction sequence (label = 1) from
 56 the high scoring matches from the reverse direction (label=0). The features used by Percolator as
 57 generally high level features of the matches, such as m/z difference between parent ion and theoretical
 58 m/z. The trained SVM is then used to clean up results from the first pass. Such a strategy can of
 59 course used even to clean up results from our methods as a second pass.

60 2 Model Components

61 We will now discuss a number of different components that we considered within our overall model
 62 family. Note that each of the four pieces above can be changed separately while adhering to the same
 63 overall structure as long as the dimension of the input and output are compatible.

64 2.1 The Fragment Representation

65 We propose two different methods of converting the amino acid representation into a fragment
 66 representation.

67 1. Trivial Representation:

68 As a baseline, we propose a trivial embedding where the amino acid representation is
 69 converted into a fragment representation via a projection. To do this we take $F : \mathbb{R}^{L \times A} \rightarrow$
 70 $\mathbb{R}^{(L+1) \times 2^A}$ defined by,

$$F(x_1, \dots, x_L) = \begin{pmatrix} x_1 & \dots & x_L & 0 \\ 0 & x_1 & \dots & x_L \end{pmatrix} \quad (1)$$

71 Thus, the fragment f_i corresponding to a breakage between amino acid $i - 1$ and i is given
 72 by the concatenation of the amino acid representation before and after the breakage.

73 2. LSTM Representation:

74 In principle, we would like the fragment representation to be able to model the fragmentation
 75 probabilities between different amino acids. However, these probabilities depend not only
 76 on the pair of amino acids on either side of the breakage point, but on the structure of the
 77 entire peptide. To this end, we propose using a deep bidirectional LSTM with K layers and
 78 hidden dimension $F/2$ to construct the fragment representation that can take into account
 79 this nonlocal information. In this case the fragment representation is defined by,

$$(z_1, \dots, z_L) = \text{Bi-LSTM}(x_1, \dots, x_L) \quad (2)$$

$$F(x_1, \dots, x_L) = \begin{pmatrix} z_1 & \dots & z_L & 0 \\ 0 & z_1 & \dots & z_L \end{pmatrix}. \quad (3)$$

80 2.2 The Spectral Representation

81 We propose two different methods of converting from the fragment representation to the spectral
 82 representation. In one case, we use theoretical knowledge about the possible ways that the peptide

83 can fragment. The other approach is agnostic to the underlying physical process. While we see
 84 significantly stronger performance when we use theory to constrain the form of our model, the
 85 agnostic approach may be more suitable when an explicit fragmentation cannot be enumerated. We
 86 also note that there is some overhead computational cost in precomputing the possible fragments.

87 1. Agnostic Representation:

88 Here we use a fully-connected network $g : \mathbb{R}^F \rightarrow \mathbb{R}^M$ to map each of the fragment
 89 representation into a corresponding contribution to the spectral representation. Thus, we
 90 write

$$Y(f_1, \dots, f_{L+1}) = \sum_{\ell} g(f_{\ell}). \quad (4)$$

91 This representation has $H = 1$ and potentially offers more interpretability since it can be
 92 normalized and interpreted as a probability distribution. Unfortunately, we were unable to get
 93 good performance using an agnostic representation that did not take explicit fragmentation
 94 patterns into account at the time of writing.

95 2. Ion Representation:

96 In this case we wish to take into account the fact that physically there are a finite number
 97 of ways in which a peptide may fragment. For each peptide we therefore enumerate all
 98 possible ways that the fragmentation can occur along with the theoretical mass-to-charge
 99 ratio that the resulting fragment will have.

100 To construct this enumeration, we first note that fragmentation occurs via the breaking of
 101 a bond between two amino acids. Moreover, between each pair of amino acids there are a
 102 number of different ways in which the fragmentation can occur (with different associated
 103 theoretical masses). In our experiments we use the three most likely breakages yielding so-
 104 called “b”, “y”, and “a” ions. Additionally fragments can have different charges associated
 105 with them. In our case we consider charges $Z = 1, 2$. Finally, can also have different
 106 neutral losses associated with them (where a molecule dissociates from the peptide during
 107 fragmentation). In our case we consider fragments that have lost an NH_3 molecule or an
 108 H_2O molecule.

109 Together this gives a combinatorial number of different ways that each breakage may occur.
 110 We enumerate these different possibilities with integers $0 \leq c \leq C \equiv 18$. For each possible
 111 breakage we construct a fully connected neural network $g_c : \mathbb{R}^F \rightarrow \mathbb{R}^H$ for some hidden
 112 dimension H . Note that since fragmentation may occur between any pair of amino acids,
 113 there are a total of $C(L - 1)$ ways that the peptide can be fragmented overall. We let m_{ic} be
 114 the mass/charge ratio of the fragment of type c that occurs between amino acid i and $i + 1$.
 115 We then define the ion representation by $G \in \mathbb{R}^{M \times H}$, where,

$$G_k = \sum_{\substack{(i,c) \\ \text{s.t.} \\ m_{ic} \in [M_k, M_{k+1}]}} g_c(f_i). \quad (5)$$

116 Note that since the total number of possible fragments is small compared to the number of
 117 m/z bins, G will typically be very sparse.

118 **2.3 Readout**

119 We consider two different readout networks.

120 1. Trivial Readout:

121 As a baseline, we consider a trivial readout where a fully-connected network is applied
 122 directly to the concatenated spectral representation. In this case the score is given by,
 123 $s = w(G)$ for some fully connected $w : \mathbb{R}^{M \times H} \rightarrow \mathbb{R}$.

124 2. VGG Readout:

125 In general, we would like our network to learn complex correlations between the empirical
 126 spectrum and the spectral representation. To that end we use a copy of the VGG network []
 127 that has been successful in computer vision models. Thus, we take $s = \text{VGG}(G)$.

128 **3 Dataset Description**

129 We consider data from a number of species taken from the ProteomeXchange database [?] containing raw spectra. In particular we considered the datasets PXD005953 (Mouse), PXD002801 (Mouse), PXD001334 (Yeast), PXD002875 (Yeast), PXD003033 (Yeast), PXD005253 (Human), and PXD003389 (Human). These datasets varied significantly in size with the smallest having around 133 30K scans and the largest having ~ 10 M scans. For each species we assemble a list of candidate peptides by direct enumeration. The size of this candidate list depends on the species in question 134 but generally varies between 1B and 10B distinct peptide sequences whose length is between 5 and 135 40. We discretize the mass spectra using bins between 100 Daltons and 2000 Daltons of width 0.5 136 Daltons. This gives us 3800 bins in our discretized mass spectrum. 137

138 **4 Network Diagnostics**

We show that both the network scores and the COMET scores display similar characteristics. To

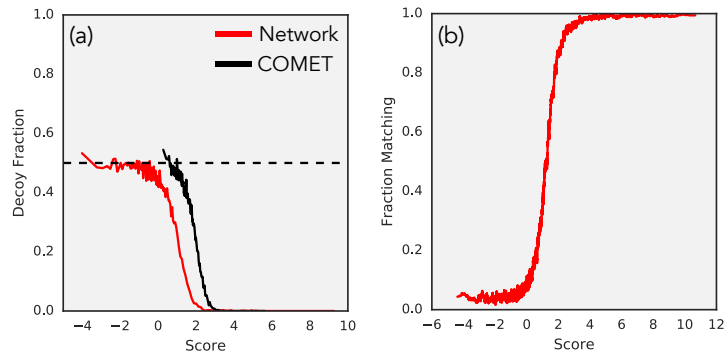


Figure 1: **Characteristics of the network scores.** (a) The fraction of decoys identified as top-1 peptide-spectra matches by the network and COMET. We see that at low scores both approach 1/2 which is shown by a dashed line. (b) The fraction of peptide-spectrum matches that have agreement between the network at COMET. We see that at high scores the two methods almost always agree.

139 this end we show, in fig. 1 (a), the decoy fraction of top-1 peptide-spectrum matches as a function 140 of the score assigned to the match. We see that we have successfully avoided selecting networks 141 that memorize peptide data since our network and COMET both approach a decoy fraction of 1/2 142 at low scores. Next, we calculate, as a function of the score, the fraction of peptide-spectrum matches 143 where the network gave the same prediction as COMET. This is shown in fig. 1 (b). We see that at 144 high scores the two assignments almost always agree. At low scores, the rate at which the two agree 145 approaches the random value. 146